Tau Decays to $3h(\pi^0)\nu$ and $5h(\pi^0)\nu$ from CLEO

W. T. Ford *

Department of Physics, University of Colorado
Boulder, Colorado 80309-0390

We present new measurements of the branching fractions $\mathcal{B}(\tau \to 3h^{\pm}(\pi^0)\nu_\tau)$, together with recently published results for $\mathcal{B}(\tau \to 5h^{\pm}(\pi^0)\nu_\tau)$. We compare these measurements with relations based upon isospin, CVC, and lattice gauge theoretical calculations.

1. INTRODUCTION

We have made new measurements of the decay branching fractions for the three- and five-prong tau decays $\tau \to 3h^{\pm}$, $3h^{\pm}\pi^0$, $5h^{\pm}$, $5h^{\pm}\pi^0$, and have obtained an upper limit for $\tau \to 5h^{\pm}2\pi^0$. Data from e^+e^- collisions at or near the $\Upsilon(4S)$ resonance, $E_{\rm cm} \sim 10.6$ GeV, were recorded with the CLEO II detector operating at the Cornell Electron Storage Ring (CESR).

The CLEO detector, described in Ref. [1], comprises a 67-layer cylindrical drift chamber system with 1.5 T solenoidal magnetic field to measure charged particle momenta, a CsI electromagnetic calorimeter to detect photons and identify electrons, and proportional tube planes interspersed with steel absorber to identify muons. Pulse height measurements in the outer 51 drift layers provide dE/dx information to further improve electron identification.

We reconstruct the tau pairs in several topologies. Leptonic decays serve as tags for all of the modes studied here. For the $\tau \to 3h^{\pm}\nu_\tau$ process we use also double 3-prong events, while for the 5-prong decays we accept non-leptonic one-prong tag decays to increase statistics. In all cases we exploit the fine-grained, high resolution electromagnetic calorimeter both to reconstruct neutral pions and to veto non-signal photons from background $q\bar{q}$ events and from unwanted tau decay modes.

Interest in measuring these modes comes from the need for consistent accounting for all of the tau decays, resolution of discrepancies among some previous measurements, and the opportunity to verify various theoretical predictions. Among the latter are isospin relations based on a_1 dominance of the 3π mode, sum rules, partially-conserved axial-vector current (PCAC) and lattice calculations of the 3 and 5 pion decay rates, and relations connecting the 4 and 6 pion decays to e^+e^- production of the corresponding charge states via the conserved vector current hypothesis (CVC).

*Work supported in part by the Department of Energy under grant DE-FG02-91ER40672.

2. THREE-PRONG MODES

We use two complementary techniques for the three-prong decay measurements. The lepton tag method is particularly clean, having low background from $q\bar{q}$ events ($e^+e^- \to q\bar{q}, q = udsc$). In the second approach we select a sample of events in which both taus decay to 3 charged tracks (3-3 sample). This method has not been used previously; advantages are that many systematic errors are reduced by a factor of two since one measures the square of the branching fraction, and the technique does not depend directly on the knowledge of any other tau decay modes (except for the estimation of the amount of "feed-across" background from other tau decay modes). The result is competitive because of the large tau pair sample and the power of the detector's photon detection capability to minimize hadronic background. Both methods require precise knowledge of the luminosity and τ-pair production cross section.

We use both methods to determine the branching fraction for the $\tau \to 3h^{\pm}\nu_\tau$ decay mode ($3h$

analysis), but only the lepton-tag method for the $\tau \to 3h^{\pm}\pi^0\nu_\tau$ decay ($3h\pi^0$ analysis). This work is described in a previous conference contribution [2].

2.1. Data sample and event selection

The total integrated luminosity of the sample is 1.58 fb^{-1}, corresponding to $\sim 1.44 \times 10^6$ produced tau-pair events. Events are selected for the lepton-tag (3-3) analysis by requiring four (six) charged tracks with the event divided into hemispheres by the charged-particle thrust axis. For the lepton-tag analysis, the leptons are required to be at least 90° from each of the 3-prong tracks. The net charge in each hemisphere is required to be ± 1 and the total charge of the event must be zero. To ensure that the event is well-reconstructed, we require the polar angle θ of all tracks to lie in the central region of the detector, $|\cos\theta| < 0.81$, and the momentum of each to be greater than $0.05E_{\rm b}$, where $E_{\rm b}$ is the beam energy. Events with secondary vertices that are consistent with K_S or Λ decays or pair conversions are rejected.

To reconstruct π^0's, we form the combined mass of the two most energetic photons with $|\cos\theta| < 0.71$. The results are shown in Fig. 1 as a plot of $(m_{\gamma\gamma} - m_{\pi^0})/\sigma_{\gamma\gamma}$. We define signal and sideband regions as $|m_{\gamma\gamma} - m_{\pi^0}| < 3.5\sigma_{\gamma\gamma}$ and $5.0\sigma_{\gamma\gamma} < |m_{\gamma\gamma} - m_{\pi^0}| < 8.5\sigma_{\gamma\gamma}$, respectively, where $m_{\gamma\gamma}$ is the mass of the photon pair and the mass resolution, $\sigma_{\gamma\gamma}$, depends on the energies and angles of the photons and is typically about 6 MeV.

To reject hadronic background and feed-across from other tau decay modes, we veto events with energetic showers which are more than 30 cm from the nearest charged track and have a lateral profile consistent with that of photons. Such events containing showers with more than 15% of the shower energy of the nearest charged hadron are rejected for the lepton-tag analysis (shower energies are such that this cut has a mean value of ~200 MeV). For the 3-3 analysis, events are vetoed if the most energetic such shower is greater than 120 MeV. These distributions are shown with the cuts indicated in Fig. 2. For the $3h\pi^0$ analysis all showers except those used for the π^0 are considered for the energetic-shower veto, and contributions due to fake π^0's are estimated from the sideband regions and subtracted.

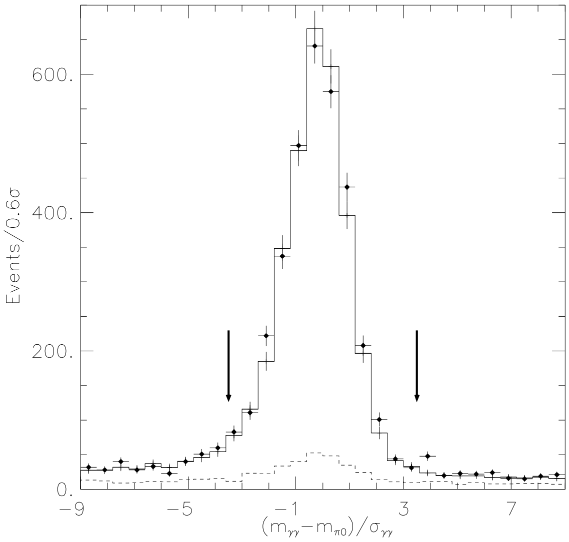

Figure 1. Invariant mass of the two candidate photons for the $3h\pi^0$ analysis. The data are shown as points with error bars, tau feed-across plus $q\bar{q}$ Monte Carlo as a dashed line and the sum of the background and signal Monte Carlo by a solid line. Arrows bracket the selected region.

For the 3-3 (lepton-tag) analysis, we reduce the hadronic background further with little loss of signal by requiring 3-prong invariant masses to be less than 1.5 GeV (1.77 GeV). The distributions are shown in Fig. 3.

For the lepton-tag analysis, we remove contamination from radiative Bhabha and muon pair events accompanied by a photon conversion by vetoing events for which the scalar sum of the momenta of the three hadron tracks exceeds $0.9E_{\rm b}$. To reject 2-photon background, we require that the polar angle of the missing momentum satisfy $|\cos\theta_{\rm miss}| < 0.90(0.98)$ for the lepton-tag (3-3) sample, and for the 3-3 analysis we require the scalar sum of the six charged-particle momenta to be at least $0.45E_{\rm cm}$. These requirements are lifted for the $3h\pi^0$ analysis, since there are no significant QED backgrounds to veto.

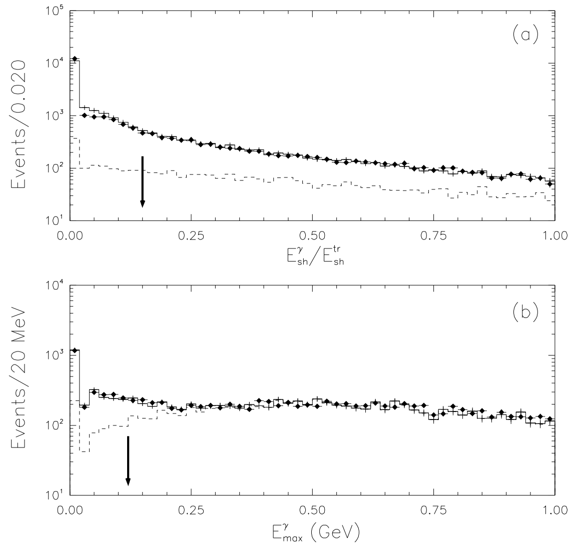

Figure 2. Energetic shower veto variables: (a) shower energy divided by the energy of the nearest charged track, used in the lepton-tag analyses; (b) energy of the most energetic photon-like shower, used in the 3-3 analysis.

The leptons in the lepton-tag cases are subject to more stringent requirements than those mentioned above. Both electrons and muons must satisfy $|\cos\theta| < 0.71$ and electrons (muons) must have momenta greater than $0.10E_{\rm b}$ $(0.26E_{\rm b})$. The momentum requirement for muons is more restrictive since muon candidates are required to penetrate at least 3 interaction lengths of iron. Electrons are required to have $E/p > 0.85$ and dE/dx within 2σ of that expected for electrons. The efficiency of lepton identification as a function of momentum is measured with radiative Bhabha and muon pair events. The probability that a hadron is misidentified as a lepton has been measured with independent tau data samples, and based on this, we determine that the final $3h$ $(3h\pi^0)$ sample contains $0.5\pm0.1\%$ $(0.6\pm0.2\%)$ fake electrons and $2.5\pm0.2\%$ $(2.8\pm0.5\%)$ fake muons.

The yields for these data samples are listed in the first column of Table 1.

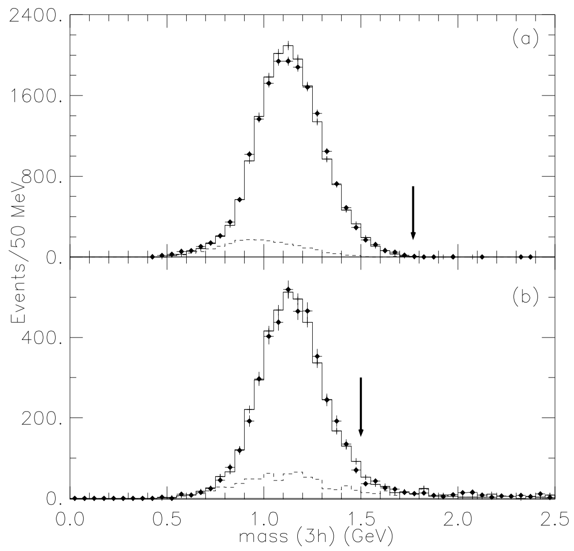

Figure 3. Distributions of $3h^{\pm}$ masses for (a) the lepton-tag $3h$ analysis; and (b) the 3-3 analysis (2 entries/event).

2.2. Efficiency and background estimation

We calculate the branching fractions from

$$\mathcal{B}(\tau \to 3h^{\pm}(\pi^0)\nu_\tau) = \frac{N_{\rm d}(1 - f_b^{q\bar{q}} - f_b^{\tau})}{2\sigma_{\tau\tau}\,\mathcal{L}\,\epsilon\,\mathcal{B}(\tau \to \ell\bar{\nu}_\ell\nu_\tau)} \quad (1)$$

for the lepton tag analysis, and

$$\mathcal{B}(\tau \to 3h^{\pm}\nu_\tau)^2 = \frac{N_d(1 - f_b^{q\bar{q}} - f_b^{\tau})}{\sigma_{\tau\tau}\,\mathcal{L}\,\epsilon} \quad (2)$$

for the 3 vs 3, where $N_{\rm d}$ is the number of data events, $f_b^{q\bar{q}}$ and f_b^{τ} are the estimated event fractions due to non-tau and tau feed-across backgrounds, respectively, $\sigma_{\tau\tau}$ is the radiatively-corrected tau cross section, $\mathcal{L}$ is the integrated luminosity and ϵ is the signal efficiency.

To determine the efficiencies and estimate backgrounds, we have generated large samples of τ-pair, $q\bar{q}$, and $B\bar{B}$ Monte Carlo. For τ-pairs we use the KORALB generator [3], for $q\bar{q}$ events the Lund Monte Carlo generator [4], and for $B\bar{B}$ events a generator developed by CLEO that is appropriate for threshold production [5]. The GEANT code [6] is used to simulate the detector response. We simulate backgrounds not associated with events from e^+e^- interactions by

Table 1
Summary of the numbers of observed events, efficiencies and background fractions.

Analysis method	$N_{\rm d}$	f_b^τ (%)	f_b^{qq} (%)	ϵ(%)
3-3	2030$\pm$ 45	10.9$\pm$1.4	4.7$\pm$0.9	12.2$\pm$0.3
e-tag $3h$	10712$\pm$103	9.6$\pm$0.5	0.2$\pm$0.2	19.1$\pm$0.6
μ-tag $3h$	6767$\pm$ 82	11.4$\pm$0.5	0.0$\pm$0.1	12.3$\pm$0.4
e-tag $3h\pi^0$	1801$\pm$ 47	6.9$\pm$0.7	0.7$\pm$0.7	7.5$\pm$0.3
μ-tag $3h\pi^0$	1146$\pm$ 37	7.2$\pm$0.7	0.3$\pm$0.3	4.9$\pm$0.2

embedding randomly triggered events into the Monte Carlo events.

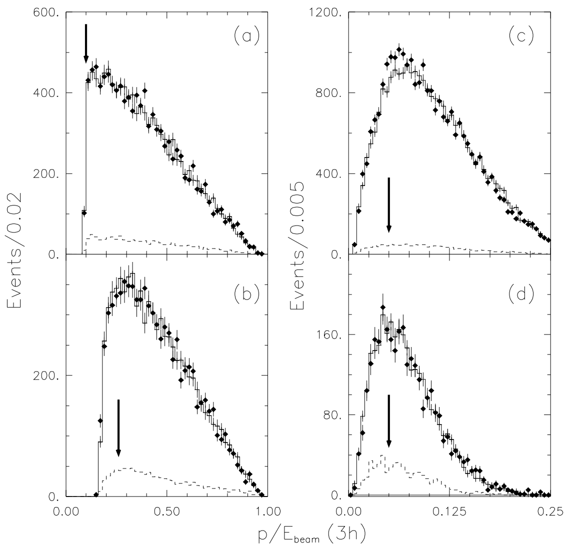

Figure 4. Distribution of momentum divided by the beam energy for (a) electrons and (b) muons from the lepton-tag $3h$ analysis; least energetic hadrons for the (c) lepton-tag $3h$ analysis and (d) 3-3 analysis. The data are shown as points with error bars, tau feed-across plus $q\bar{q}$ Monte Carlo as a dashed line and the sum of the background and signal Monte Carlo by a solid line. Arrows indicate the location of the selection cuts.

We have compared the data and Monte Carlo distributions for many quantities, including those used in the event selection, and find good agreement for nearly all. As examples, we show in Fig. 4 distributions of the lepton momenta and the smallest hadron momentum in the event for both analyses. The disagreement near the peak in Fig. 4c is thought to be a fluctuation in the data, but it is taken into account in the systematic errors in any case. The $3h^\pm$ masses for the two analyses are shown in Fig. 3. The plots include all cuts except those on the quantity being plotted.

Similar plots for the $3h\pi^0$ analysis also show good consistency of data with Monte Carlo. Momentum plots for the leptons and least energetic hadron are shown in Fig. 5.

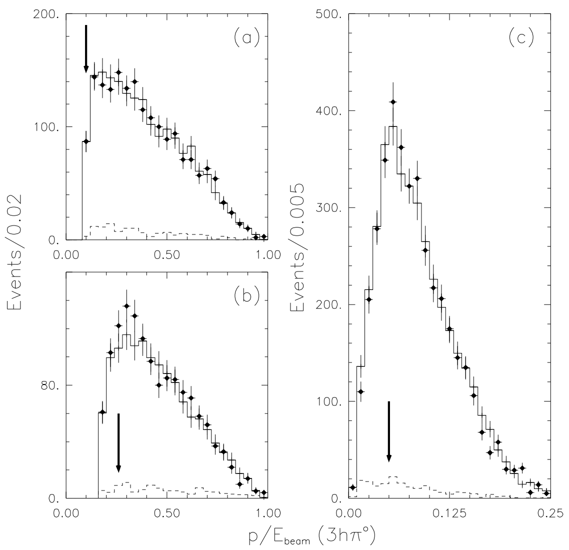

Figure 5. Distribution of momentum divided by the beam energy for (a) electrons and (b) muons from the $3h\pi^0$ analysis; (c) least energetic hadron from the same analysis.

For the 3-3 analysis, we estimate the amount of $q\bar{q}$ background from the Monte Carlo, scaled up by a factor of 1.2 ± 0.2 to agree with the number of events in the mass region between 1.5 and 2.0 GeV. Other variables which are sensitive to hadronic background are in good agreement with this estimate. With this adjustment, we estimate the amount of $q\bar{q}$ background to be $4.7 \pm 0.9\%$, where the uncertainty is dominated by that of the scale factor mentioned above. We estimate that the residual 2-photon background is negligible from distributions sensitive to this background other than those used in the analysis. The amount of $B\bar{B}$ is estimated from a large Monte Carlo sample and found to be negligible. With similar techniques, all of these backgrounds are estimated for the lepton-tag analysis and all but the $q\bar{q}$ background are estimated to be negligible.

The largest background comes from feed-across of other tau decays into the signal sample (generally feed-down from modes with more π^0's. For the 3-3 analysis we use the τ Monte Carlo and comparisons with the data mass and unassociated-neutral-energy distributions to estimate this background to be $10.9\pm 1.4\%$, where 86% of the background is from the $\tau \to 3h^{\pm}\pi^0\nu_\tau$ decay mode. For the lepton-tag $3h$ sample, we estimate the feed-across to be $9.6\pm 0.5\%$ and $11.4\pm 0.5\%$ for the electron-tag and muon-tag samples, respectively. The feed-across includes the lepton-fake contributions given above. About 80% of the cross-feed in the signal hemisphere is from the $\tau \to 3h^{\pm}\pi^0\nu_\tau$ decay mode. For the $3h\pi^0$ analysis, the feed-across background is estimated to be $6.9\pm 0.7\%$ and $7.2\pm 0.7\%$ for the electron- and muon-tag samples, respectively. This background is dominated by the decay $\tau \to 3h^{\pm}2\pi^0\nu_\tau$.

2.3. Results for $3h(\pi^0)$

We calculate the branching fractions from eq (1) for the lepton tag analysis, and eq (2) for the 3 vs 3. The signal efficiency is calculated from Monte Carlo as discussed above. For $\mathcal{B}(\tau \to \ell\bar{\nu}_\ell\nu_\tau)$, we use the world averages from Ref. [7].

The relevant information for the calculation can be found in Table 1. We calculate the cross section, with a precision of 1%, using KORALB. It is the point cross section (0.779 nb at our average center-of-mass energy) times an order α^3 radiative-correction factor, 1.173. We determine the luminosity with a precision of 1% by using events from the processes $e^+e^- \to e^+e^-$, $e^+e^- \to \gamma\gamma$ and $e^+e^- \to \mu^+\mu^-$, all in the region $|\cos\theta| < 0.71$ [8]. We find the branching fraction results given in Table 2, where the first uncertainties are statistical and the second systematic.

We have considered a variety of systematic errors, summarized in Table 3. The systematic error for the absolute tracking efficiency is conservatively determined by studying a sample of electron-tagged events with 1-2 and 1-3 topology. These decays are predominantly 3-prong tau decays, and in about 94% of the events, all three tracks are reconstructed; the variation of this number as requirements are changed provides the systematic error estimate of 0.65% per track. The systematic error due to tau backgrounds includes the uncertainty in tau branching fractions. Since the efficiency of the $3h$ analyses is estimated to be $\sim$15% larger for modes with charged kaons, uncertainties in the branching fractions of the decays $\tau^- \to K^-\pi^+\pi^-\nu_\tau$ and $\tau^- \to K^-K^+\pi^-\nu_\tau$ have been included in the systematic error [9]. We determined the uncertainty in the efficiency by varying all selection criteria and adding in quadrature estimates of the variation due to each of them. The electron identification uncertainty was determined from studies of radiative Bhabha-scattering events; the muon identification uncertainty was determined from radiative μ-pair events and by variation of the requirement on the depth of muon penetration. The uncertainty in the absolute efficiency for π^0 reconstruction is conservatively taken to be three times the error assigned in the measurement of the decay $\tau \to h^{\pm}\pi^0\nu_\tau$[10], accounting for a possible increase due to the three tracks in the signal hemisphere. Note that in Table 3, we have given uncertainties in the branching fraction, not the number of events; for the 3-3 analysis, these uncertainties have benefited from the factor of two reduction discussed in the introduction.

In order to combine the $3h$ results shown in Table 2, we determine the correlated and uncorrelated systematic errors for each measurement.

Table 2
Summary of branching fraction measurements.

Analysis method	$\mathcal{B}(\tau \to 3h^\pm \nu_\tau)$	$\mathcal{B}(\tau \to 3h^\pm \pi^0 \nu_\tau)$
3-3	0.0985$\pm$0.0014$\pm$0.0033	-
e-tag $3h$	0.0981$\pm$0.0011$\pm$0.0043	0.0427$\pm$0.0011$\pm$0.0025
μ-tag $3h$	0.0974$\pm$0.0013$\pm$0.0045	0.0423$\pm$0.0014$\pm$0.0026

Table 3
Summary of systematic uncertainties in the measured $\mathcal{B}$'s (%).

Source	3-3	e-tag $3h$	μ-tag $3h$	e-tag $3h\pi^0$	μ-tag $3h\pi^0$
Luminosity	0.5	1.0	1.0	1.0	1.0
Tau cross section	0.5	1.0	1.0	1.0	1.0
Tracking efficiency	2.0	2.5	2.5	2.5	2.5
Non-tau backgrounds	0.5	1.0	0.5	0.6	0.8
Tau backgrounds	0.7	0.5		0.7	
Efficiency (cut variation)	2.2	3.2		4.1	4.8
Monte Carlo statistics	0.8	0.6	0.7	0.9	1.2
Lepton ID	-	0.2	1.0	0.2	1.0
$\mathcal{B}(\tau \to \ell\bar{\nu}_\ell\nu_\tau)$	-	1.0	1.3	1.0	1.3
π^0 reconstruction	-	-	-	3.0	
Total	3.3	4.6	4.7	6.1	6.7

The statistical and uncorrelated systematic errors are used to form weights, and a combined branching fraction is determined from the weighted average of the two results. We obtain the combined error by summing in quadrature the error in this weighted average and the weighted linear sum of the correlated errors. The weights are 0.63 for the 3-3 measurement and 0.37 for the lepton-tag measurement, leading to a combined result

$$\mathcal{B}(\tau \to 3h^\pm \nu_\tau) = 0.0982 \pm 0.0009 \pm 0.0034.$$

By a similar procedure we combine the electron- and muon-tag measurements in the $3h\pi^0$ analysis. The result is

$$\mathcal{B}(\tau \to 3h^\pm \pi^0 \nu_\tau) = 0.0425 \pm 0.0009 \pm 0.0026.$$

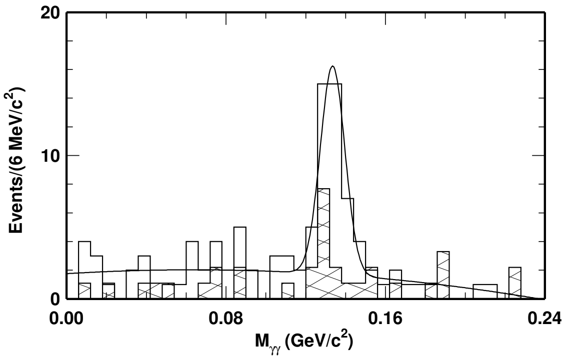

Figure 6. Distribution of photon pair masses for the $5h\pi^0$ candidates. Shaded histogram shows the hadronic background.

3. FIVE-PRONG MODES

The five-prong tau decay modes are highly suppressed by phase space, and are less readily distinguished from multihadron events. To measure these modes we depend upon background estimates based on high mass jets in the data. This work is already published [11].

We select candidates having six charged tracks of zero net charge. Each must be reconstructed in the detector's central region $|\cos\theta| < 0.90$ and point back the the interaction region. Reconstructed K_S's and photon conversions are removed. We require a 1 vs 5 topology defined in terms of projections onto the thrust axis. Photons and π^0's are reconstructed from calorimeter data as in the 3-prong analysis. The $\gamma\gamma$ mass distribution for the $5h^\pm\pi^0$ candidates is shown in Fig. 6.

For the one-prong tag we limit the number of neutrals to zero or one photon or one reconstructed π^0. The one(five)-prong mass must be less than 1.2(1.7) GeV/c^2, and in the 5-prong hemisphere the apparent neutrino mass squared must be positive. A subset of events in which the 1-prong hemisphere is required to contain a lepton is examined separately to help understand the background.

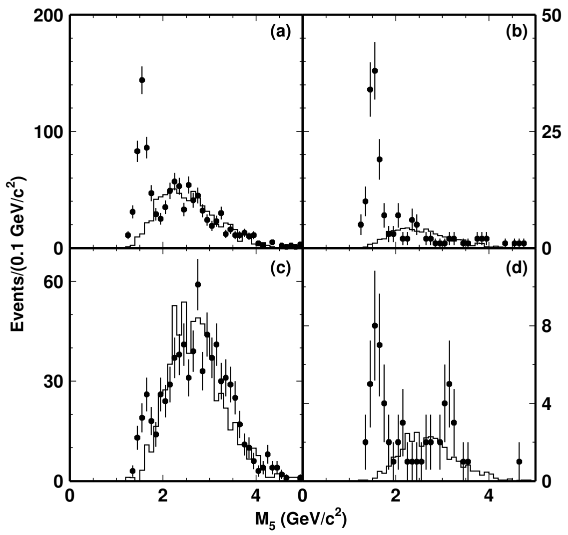

Figure 7. Mass spectra of the (a) $5h^\pm$ and (c) $5h^\pm\pi^0$ candidates selected with the 1-prong tag. The M_ν cut, which suppresses the hadronic background by $\sim$ 50%, has been removed because it is unphysical for $M_5 > M_\tau$. The histograms show the hadronic background, normalized for $M_5 > 2.0$ GeV/c^2. (b) and (d) are the corresponding spectra selected with the lepton tags.

The data, with the M_5 and M_ν cuts removed, are shown in Fig. 7. A clear peak for $5h^\pm(\pi^0)$ masses below M_τ is evident. The histograms show background events, selected with the requirement $1.7 < M_1 < 2.5$ GeV/c^2 and normalized to the data ($M_1 < 1.2$ GeV/c^2) over the range $M_5 > 2.0$ GeV/c^2.

We calculate the 5-prong branching fractions from eq (1), replacing the leptonic branching fraction by the branching fraction summed over modes contributing to the one-prong tags. The results are

$$\begin{aligned}
\mathcal{B}(\tau \rightarrow 5h^\pm\nu_\tau) &= (0.077 \pm 0.005 \pm 0.009)\% \\
\mathcal{B}(\tau \rightarrow 5h^\pm\pi^0\nu_\tau) &= (0.019 \pm 0.004 \pm 0.004)\% \\
\mathcal{B}(\tau \rightarrow 5h^\pm 2\pi^0\nu_\tau) &< 0.011\%, \text{ at } 90\% \text{ C.L.}
\end{aligned}$$

These are are consistent with the corresponding world averages [7].

4. DISCUSSION

4.1. 3- and 5-pion (axial vector) decays

The three pion state is expected to be dominated by the $a_1(1260)$ resonance. The Monte Carlo calculation we have used contains this assumption, and one can see good agreement between Monte Carlo and data in the mass spectra of Fig. 3, as pointed out previously. By isospin this implies equality between the $\pi^\pm\pi^+\pi^-$ and $\pi^\pm 2\pi^0$ modes, modified slightly by a phase space factor [3]:

$$\mathcal{B}(\tau \rightarrow \pi^\pm\pi^+\pi^-\nu_\tau) = 0.98\mathcal{B}(\tau \rightarrow \pi^\pm 2\pi^0\nu_\tau). \quad (3)$$

To extract a value for the left-hand side we take the CLEO number from sect. 2.3 for $\mathcal{B}(3h^\pm\nu_\tau)$ and subtract the contributions from $K\pi\pi$ and $KK\pi$, using world averages [12] from Ref. [13]. For the right-hand side we start with CLEO's measurements $\mathcal{B}(h2\pi^0/h\pi^0) = 0.345 \pm 0.006 \pm 0.016$ [14] times $\mathcal{B}(h\pi^0) = (25.87 \pm 0.12 \pm 0.42)\%$ [10], and subtract the $K2\pi^0$ contribution [12]. The results are

$$\begin{aligned}
\mathcal{B}(\tau \rightarrow \pi^\pm\pi^+\pi^-\nu) &= (9.1 \pm 0.4)\% \\
\mathcal{B}(\tau \rightarrow \pi^\pm 2\pi^0\nu) &= (8.8 \pm 0.5)\% \\
0.98\mathcal{B}(\tau \rightarrow \pi^\pm 2\pi^0\nu) &= (8.7 \pm 0.5)\%.
\end{aligned}$$

The comparison of the first and third lines shows consistency with the isospin prediction, eq (3), for the $a_1(1260)$. The total 3π ($\simeq a_1$) branching fraction is

$$\mathcal{B}(\tau \rightarrow a_1\nu_\tau) = (17.9 \pm 0.7)\%.$$

Theoretical calculations of the branching fraction may be cast in terms of the decay constant f_{a_1}, defined by

$$\langle 0|A_\mu|a_1\rangle = \epsilon_\mu f_{a_1},$$

with A_μ the axial-vector hadronic current, and ϵ_μ the polarization vector. In this notation the narrow width limit of the spectral function is [15]

$$a_1(q^2) = 2\pi \left(\frac{f_{a_1}}{m_{a_1}}\right)^2 \delta(q^2 - m_{a_1}^2),$$

and the decay width is

$$\Gamma(\tau \to a_1\nu_\tau) = \frac{G_F^2|V_{ud}|^2}{32\pi^2 m_\tau^3} \int_0^{(m_\tau - m_{\nu_\tau})^2} dq^2 \times (m_\tau^2 - q^2)^2(m_\tau^2 + 2q^2)a_1(q^2).$$

A new lattice gauge theory calculation [16] gives $f_{a_1} = 0.281 \pm 0.037$ GeV^2. The problem of converting this to a decay rate is complicated by the large width of the a_1 and of the intermediate ρ mesons in the decay to three pions. (The narrow width approximation given above is in no way adequate.) The rate and the spectral function $a_1(q^2)$ have been extracted [17] from fits to earlier data for the branching fraction and $3h^\pm$ mass spectrum to obtain $f_{a_1} = 0.25 \pm 0.02$ GeV^2, which agrees with the lattice prediction. One would like to update this result with the new branching fraction measurements, but f_{a_1} cannot be scaled in a straightforward fashion from the information contained in Ref. [17].

Turning to the 5 pion decays, we combine our result for $\mathcal{B}(\tau \to 5h^\pm\nu_\tau)$ with CLEO measurements for $\mathcal{B}(\tau \to h^\pm 4\pi^0\nu_\tau)$ [14] and $\mathcal{B}(\tau \to 3h^\pm 2\pi^0\nu_\tau)$ [24] to obtain the five pion fraction (all charge states, assuming $h \simeq \pi$)

$$\mathcal{B}(\tau \to 5\pi) = (0.61 \pm 0.06 \pm 0.08)\%.$$

The prediction [20] from PCAC is $\sim 1\%$.

The spectral function $a_1(q^2)$ introduced above more generally includes higher-mass axial vector meson resonances than $a_1(1260)$, such as the spin-1 part of the 5 pion state, although these will be suppressed by phase space in tau decays. Similarly the vector counterpart $v_1(q^2)$ contains non-negligible contributions from 4 pion states, in addition to the leading $\rho(770)$ part. The spectral functions are related through sum rules derived by Weinberg [18] from current algebra, which in more modern terms represent the chiral limit of QCD. With f_π the pion decay constant, these are

$$\int_0^\infty \left[v_1(q^2) - a_1(q^2)\right] dq^2 = 2\pi f_\pi^2$$

and

$$\int_0^\infty q^2 \left[v_1(q^2) - a_1(q^2)\right] dq^2 = 0.$$

Note that the integrals run to infinity in q^2, while tau decay data cut off at m_τ^2. These relations have been studied in detail by Peccei and Solà [19], who find, modulo the cutoff ambiguities, reasonable consistency of the first rule with 1986 ARGUS data [19]. They see some disagreement with the second (which as Marciano has pointed out at this workshop, is less well behaved because of the q^2 weighting). This problem deserves to be revisited with today's data; in particular, the a_1 branching ratio used was $2 \times 5.6\%$, considerably below the recent measurements.

4.2. 4- and 6-pion (vector) decays

Our measurement of $\mathcal{B}(\tau \to 3\pi^\pm\pi^0\nu_\tau) = (4.25 \pm 0.09 \pm 0.26)\%$ (taking $h \simeq \pi$) compares with predictions [21] via CVC from e^+e^- data of $(4.20 \pm 0.29)\%$. The mass spectrum of the $3h^\pm\pi^0$ system given in Fig. 8 shows good agreement with the parameterized e^+e^- data [3]. (The e^+e^- data also have substantial errors, not shown).

In Fig. 9 we show the masses of the $\pi^+\pi^-\pi^0$ combinations and the three two pion combinations. The Monte Carlo distribution is also shown [22]. An ω resonance is evident, and indications of ρ mass peaks are seen in each charge combination. Quantitative studies of the Dalitz plot of this decay mode are in progress.

Our measurement $\mathcal{B}(\tau \to 5\pi^\pm\pi^0\nu_\tau) = (0.019 \pm 0.004 \pm 0.004)\%$ is related to the total 6 pion fraction by the isospin bounds [23]

$$\frac{1}{5} \le \frac{\mathcal{B}(\tau \to 5\pi^\pm\pi^0\nu_\tau)}{\mathcal{B}(\tau \to (\text{all } 6\pi)\nu_\tau)} \le \frac{4}{5}.$$

This in combination with data from e^+e^- production of 6 pions and CVC thus predict the lower bound [21]

$$\mathcal{B}(\tau \to 5\pi^\pm\pi^0\nu_\tau) \ge (0.027 \pm 0.005)\%,$$

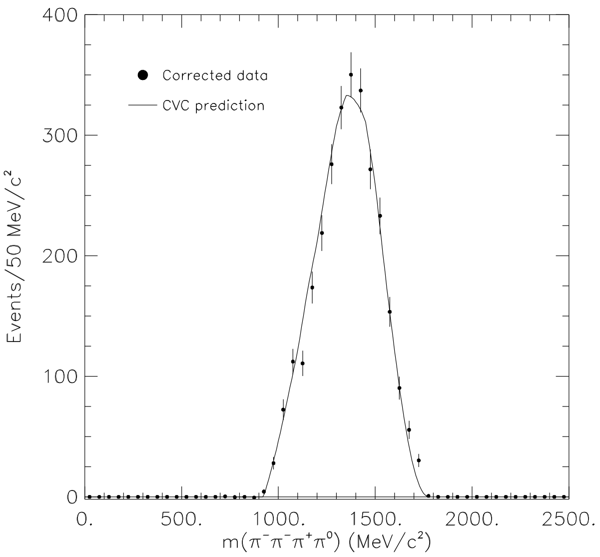

Figure 8. Distributions of $3h^{\pm}\pi^0$ effective mass for the CLEO data, corrected for background and efficiency, compared with the CVC prediction normalized in area to the data.

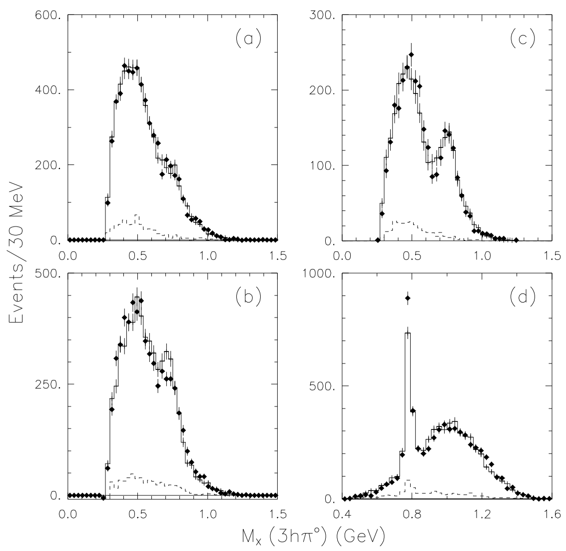

Figure 9. Distributions of sub-masses, M_X, for the $3h\pi^0$ analysis: (a) $\pi^+\pi^-$; (b) $\pi^-\pi^0$; (c) $\pi^+\pi^0$; (d) $\pi^+\pi^-\pi^0$ final states, where these final states are for a τ^- decay, but charge-conjugate final states are also included. All plots except (c) have two entries/event and (c) has one entry/event.

not inconsistent with the measurement. The shapes of the six pion spectra are compared in Fig. 10, where we observe agreement within the rather large errors.

4.3. Inclusive 3- and 5-prong fractions

By combining the $3h^{\pm}$ and $3h^{\pm}\pi^0$ measurements presented in this paper with the CLEO measurement for the $\tau \to 3h^{\pm}2\pi^0\nu_\tau$ decay mode [24] and the recent ALEPH measurement [25] of $\tau \to 3h^{\pm}(\geq 3)\pi^0$, we determine the inclusive 3-prong branching fraction to be

$$\mathcal{B}_3 = 0.1475 \pm 0.0013 \pm 0.0059.$$

Again, this result specifically excludes contributions from decay modes involving K^0 decays. It is in good agreement with other recent measurements of $\mathcal{B}_3$ and the world average, $\mathcal{B}_3$=0.1432$\pm$0.0027 [7].

Summing the 5-prong measurements (sect. 3) gives the inclusive branching fraction

$$\mathcal{B}_5 = (0.097 \pm 0.005 \pm 0.011)\%.$$

5. CONCLUSIONS

We have measured the branching fractions

$$\begin{aligned}
\mathcal{B}(\tau \to 3h^{\pm}\nu_\tau) &= (9.82 \pm 0.09 \pm 0.34)\% \\
\mathcal{B}(\tau \to 3h^{\pm}\pi^0\nu_\tau) &= (4.25 \pm 0.09 \pm 0.26)\% \\
\mathcal{B}(\tau \to 5h^{\pm}\nu_\tau) &= (0.077 \pm 0.005 \pm 0.009)\% \\
\mathcal{B}(\tau \to 5h^{\pm}\pi^0\nu_\tau) &= (0.019 \pm 0.004 \pm 0.004)\% \\
\mathcal{B}(\tau \to 5h^{\pm}2\pi^0\nu_\tau) &< 0.011\%, \text{ at } 90\% \text{ C.L.}
\end{aligned}$$

A review of these and other new measurements in comparison with previous results is contained in the contribution of Brian Heltsley to these proceedings [13].

ACKNOWLEDGEMENTS

I've received the benefit of discussions with theory colleagues Tom DeGrand and Matt Wingate, and with my CLEO collaborators, especially Jim Smith, Martin Lohner, Tomasz Skwarnicki, Vasilii Shelkov, Ryszard Stroynowski, Brian Helt-

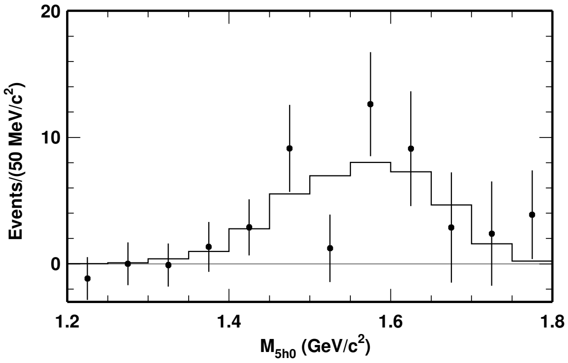

Figure 10. Mass distribution for the $5\pi\pi^0$ final state, compared with the charge conjugate 6 pion state produced in e^+e^- annihilations.

sley, Alan Weinstein, and K. K. Gan.

REFERENCES

1. Y. Kubota *et al.* (CLEO collaboration), Nucl. Instrum. Methods Phys. Res., Sect. A **320**, 66(1992).
2. B. Barish *et al.* (CLEO collaboration), contributed to XXVII International Conference on High Energy Physics, Glasgow, Scotland (1994), Ref. GLS0249 (CLEO CONF 94-22).
3. KORALB (v.2.1) / TAUOLA (v.1.5): S. Jadach and Z. Was, Comput. Phys. Commun. **36**, 191 (1985); **64**, 267 (1991); S. Jadach, J. H. Kühn, and Z. Was, Comput. Phys. Commun. **64**, 275 (1991); **70**, 69 (1992); **76**, 361 (1993).
4. JETSET 7.3: T. Sjöstrand and M. Bengtsson, Comput. Phys. Commun. **43**, 367 (1987).
5. P. Avery, K. Read and G. Trahern, CLEO internal note CSN-212.
6. R. Brun *et al.*, GEANT 3.15, CERN DD/EE/84-1.
7. L. Montanet *et al.* (Particle Data Group), Phys. Rev. D **50**, 1173 (1994).
8. G. Crawford *et al.* (CLEO collaboration), Nucl. Instrum. Methods Phys. Res., Sect. A **345**, 429 (1994).
9. We use world-average branching fractions for these modes: $\mathcal{B}(\tau^- \to K^-\pi^+\pi^-\nu_\tau)$= 0.0037$\pm$0.0010 and $\mathcal{B}(\tau^- \to K^-K^+\pi^-\nu_\tau)$= 0.0013$\pm$0.0003. These branching fractions were obtained by averaging the results given in Ref. [7] with more recent ones: D. A. Bauer *et al.* (TPC/2γ collaboration), Phys. Rev. D **50** R13 (1994); C. Hast (ARGUS collaboration) 1994 Rencontres de Moriond, Les Arcs, France (March 1994).
10. M. Artuso *et al.* (CLEO collaboration), Phys. Rev. Lett. **73**, 3762 (1994).
11. D. Gibaut *et al.* (CLEO collaboration), Phys. Rev. Letters **73**, 934 (1994).
12. The kaonic branching fractions subtracted to obtain the pure pionic ones are (in %) $\mathcal{B}(K\pi\pi\nu) = 0.48 \pm 0.10$, $\mathcal{B}(KK\pi\nu) = 0.20 \pm 0.06$, and $\mathcal{B}(K2\pi^0\nu) = 0.09 \pm 0.03$.
13. B. Heltsley, presented at this workshop.
14. M. Procario *et al.* (CLEO collaboration), Phys. Rev. Lett. **70**, 1207 (1993).
15. Y-S. Tsai, Phys. Rev. D **4**, 2821 (1971).
16. M. Wingate, T. DeGrand, S. Collins, and U. Heller, Poster submitted to the Lattice94 Workshop, Bielefeld, Germany (1994).
17. N. Isgur, C. Morningstar, and C. Reader, Phys. Rev. D **39**, 1357 (1989).
18. S. Weinberg, Phys. Rev. Letters **18**, 507 (1967). We follow Ref. [15] for the notation.
19. R. D. Peccei and J. Solà, Nuclear Physics **B281**, 1 (1987); data from H. Albrecht *et al.* (ARGUS collaboration), preprint DESY-86-060.
20. T. N. Pham, C. Roiesnel, and T. N Truong, Phys. Letters **B78**, 623 (1978).
21. S. I. Eidelman, presented at this workshop; S. I. Eidelman and V. N. Ivanchenko, Phys. Letters **B257**, 437 (1991).
22. The KORALB relative amplitudes for the $\omega\pi$ and the three $\rho\pi$ combinations were tuned to obtain agreement with the data.
23. F. J. Gilman and S. H. Rhie, Phys. Rev. D **31**, 1066 (1985).
24. D. Bortoletto *et al.* (CLEO collaboration), Phys. Rev. Lett. **71**, 1791 (1993).
25. M. Girone, presented at this workshop.